Serial Silver Clusters Biomineralized by One Peptide

Yanyan Cui,[§] Yaling Wang,[§] Ru Liu, Zhipeng Sun, Yueteng Wei, Yuliang Zhao, and Xueyun Gao*

Lab for Biomedical Effects of Nanomaterials and Nanosafety, Institute of High Energy Physics, Chinese Academy of Sciences, Beijing 100049, People's Republic of China [§]These authors contributed equally to this work.

ABSTRACT

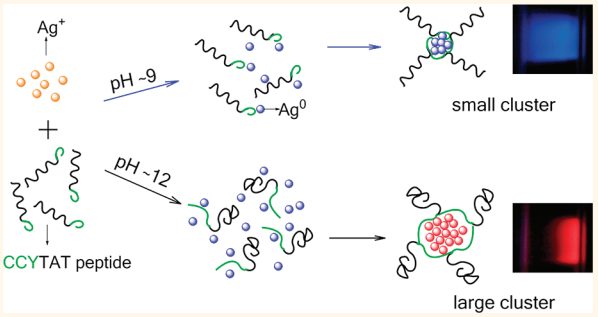

The artificial peptide with amino acid sequence CCYRGRKKRRQRRR was used to biomineralize serial Ag clusters. Under different alkaline conditions, clusters with red and blue emission were biomineralized by the peptide, respectively. The matrix-assisted laser desorption/ionization time-of-flight mass spectra implied that the red-emitting cluster sample was composed of Ag_{28}, while the blue-emitting cluster sample was composed of Ag_5, Ag_6, and Ag_7. The UV—visible absorption and infrared spectra revealed that the peptide phenol moiety reduced Ag^+ ions and that formed Ag clusters were captured by peptide thiol moieties. The phenol reduction potential was controlled by the alkalinity and played an important role in determining the Ag cluster size. Circular dichroism observations suggested that the alkalinity tuned the peptide secondary structure, which may also affect the Ag cluster size.

KEYWORDS: silver cluster · peptide · biomineralization · reduction potential · secondary structure

Noble metal clusters are collections of two to tens of atoms of gold or silver with radii less than the Fermi wavelength of the electron (0.5 nm for Au or Ag).[1] They were small enough to preclude the continuous density of states of the bulk. The clusters have a discrete electronic state and exhibit strong size-dependent fluorescence over the region from ultraviolet to near infared.[2] These excellent fluorescence properties of clusters were suitable for chemical sensing, bioimaging, and single-molecule studies.[3−11] Au clusters have been studied for decades, and many Au clusters with well-defined composition such as Au_8,[12] Au_{13},[13] Au_{25},[14,15] and Au_{38}[16] have been reported. Some small molecular Ag clusters exhibit size-dependent wavelength emission within rare gas matrixes,[17] on silver oxide surfaces,[18] and in aqueous solution. Some soft landing such as arylthiolates,[19] oligonucleotides,[20−24] dendrimers,[2,25,26] and peptides[27,28] enable us to synthesis Ag clusters in water solution. Many reported Au clusters were monosized and with distinct molecular composition, while for the Ag cluster, only a few (Ag_7, Ag_9) monodispersed products were obtained, because such size control in aqueous solutions is greatly complicated by aggregation and reactivity. Clusters from these approaches have generally been produced from Ag^+ and strong reducing agents such as $NaBH_4$, with the organic molecule capping the final cluster. Strong reducing agents can potentially have side effects when the organic molecule—cluster hybrids are used in biologic applications.[29] Many biomimetic methods have recently been developed to prepare nanomaterials[30−34] through the use of green reducing agents and biomimetic ligands.[34] However, there are no reported biomimetic approaches for precisely producing metal clusters using peptides.

In the current study, we have designed an artificial peptide with the amino acid sequence CCYRGRKKRRQRRR to biomineralize Ag clusters. Serial Ag clusters were biomineralized and anchored *via* this peptide *in situ* under different pH conditions, and no adventitious reducing agents were used. In addition to the biomineralization function, this peptide possesses cell-targeting ability owing to its nucleus localization signal sequence derived from the protein HIV-1 TAT.[35−38] This approach opens new pathways for preparing versatile fluorescent peptide—clusters with potential applications in cellular staining, bioimaging, and single-molecule studies.

RESULTS AND DISCUSSION

The peptide H_2N-CCYRGRKKRRQRRR-COOH (abbreviated as *CCYTAT*), containing two domains, was designed. Domains 1 and 2 are CCY and RGRKKRRQRRR, respectively.

* Address correspondence to gaoxy@ihep.ac.cn.

Received for review July 10, 2011 and accepted October 24, 2011.

Published online October 24, 2011
10.1021/nn202566n

Domain 1 can reduce Ag^+ into Ag clusters *via* the phenolic group of tyrosine (*Y*) under alkaline conditions and capture the clusters *via* the SH group of cysteine (*C*). Domain 2 is a nucleus localization signal sequence derived from the protein HIV-1 TAT and possesses nucleus-targeting ability.[35−38] The *CCYTAT* peptide can biomineralize Ag^+ *in situ* and form blue or red fluorescent Ag clusters by adjustment of the pH (Scheme 1).

Obtaining discrete fluorescence of the Ag cluster samples was an important goal. The fluorescence

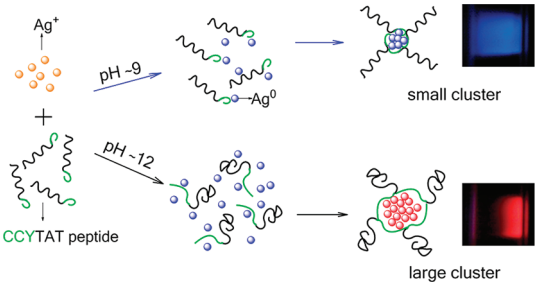

Scheme 1. Illustration of peptide−Ag cluster formation. The peptide can biomineralize Ag^+ *in situ* and produce Ag clusters in aqueous solution. At pH values of ~9 and ~12, Ag clusters with blue and red emission are formed, respectively. Red- and blue-emitting clusters are denoted *C-1* and *C-2*, respectively.

spectra in Figure 1 show that the as-synthesized *C-1* and *C-2* Ag clusters exhibit red and blue emission, respectively. *C-1* (Figure 1a) shows an emission peak at 661 nm when excited at 607 nm, and *C-2* (Figure 1b) shows an emission peak at 432 nm when excited at 347 nm. The digital photos were obtained upon 365 nm Xe arc lamp excitation (Figure 1, insets). The quantum yields of *C-1* and *C-2* were about 0.8% and 1.5%, using sulforhodamine 101 and quinine hemisulfate monohydrate as reference agents, respectively. Details of the fluorescence characterization and the quantum yield measurement are available in Supporting Information section S1.

Accurately identifying the mass of the Ag clusters may help to understand the correlation between size and emission, and matrix-assisted laser desorption/ionization time-of-flight mass spectrometry (MALDI-TOF MS) is the conventional method for achieving this.[39−41] It can accurately provide the number of Ag and peptide moieties of single Ag cluster−peptide hybrids. MALDI-TOF MS studies of *C-1* and *C-2* (Figure 2) were performed in positive ion mode using α-cyano-4-hydroxycinnamic acid (CHCA) as a matrix. Detailed methodology is available in Supporting Information section S2.

For *C-1* (Figure 2a), the most abundant *m/z* peak at 3725 Da is assigned to $Ag_{28}S_{22}^+$, confirmed by the

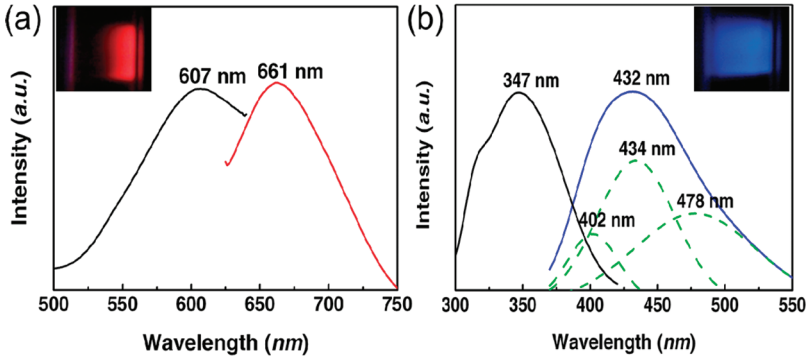

Figure 1. Photoluminescence spectra and photographic images of *C-1* and *C-2*. (a) Emission of *C-1* at 661 nm (red) excited at 607 nm (black). (b) Emission of *C-2* at 432 nm (blue) excited at 347 nm (black). The emission spectrum of *C-2* was fitted by a Gaussian method, and the three component peaks at 402, 434, and 478 nm (green) are shown. The insets in (a) and (b) are emission images of *C-1* and *C-2*, respectively, upon illumination with a Xe arc lamp at 365 nm excitation.

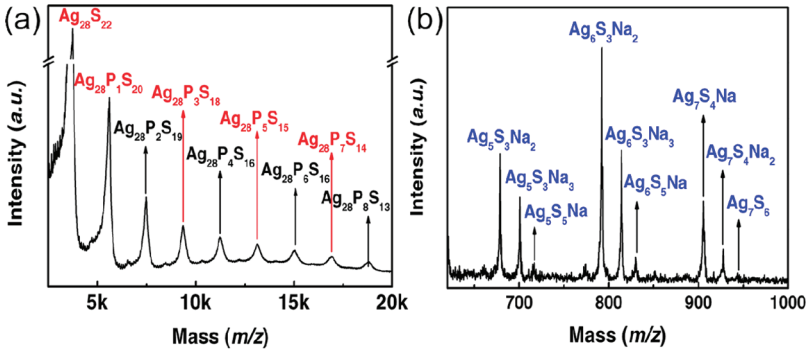

Figure 2. MALDI-TOF mass spectra of *C-1* and *C-2*. (a) The core mass is $Ag_{28}P_mS_n$ (where P is *CCYTAT*, $m = 0-8$, $n = 13-22$), and the highest signal is assigned to $Ag_{28}S_{22}^+$. The spacing between adjacent *m/z* peaks is consistent with a peptide of 1923 Da. (b) The *m/z* peaks are consistent with $Ag_xS_yNa_z$ ($x = 5, 6, 7$; $y = 3-6$; $z = 0-6$). Data were acquired using the linear model.

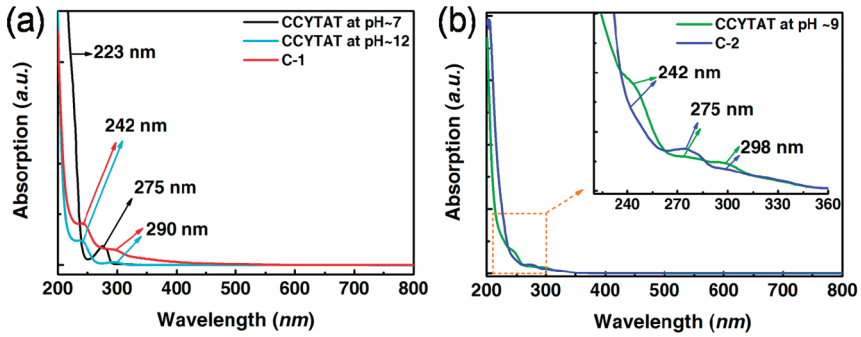

Figure 3. (a) Absorption spectra of *C-1* (red) and *CCYTAT* solution at pH ~7 (black) and ~12 (cyan). The *CCYTAT* absorption peaks at pH ~7 are at 223 and 275 nm. At pH ~12, the *CCYTAT* and *C-1* solutions have similar absorptions at 242 and 290 nm. (b) Absorption spectra of *C-2* (blue) and *CCYTAT* at pH ~9 (green), which have similar absorptions at 223, 242, 275, and 298 nm.

excellent match to the theoretical isotopic pattern (Figure S2a). There are also weaker serial peaks ($Ag_{23}S_{19}^{+}$–$Ag_{28}S_{21}^{+}$) below 3725 Da (Figure S2b), which may be derived from the fragmentation of $Ag_{28}S_{22}^{+}$ in the desorption/ionization process.[40] In the 5–20K *m/z* region (Figure 2a), a series of peaks are present, *e.g.*, $Ag_{28}P_mS_n$, where the spacing between adjacent *m/z* peaks is close to the mass of one *CCYTAT* (1923 Da). The S attached to the Ag cluster originates from the peptide, as the C–S bond of the peptide is easily broken during the MALDI-TOF desorption/ionization process (Figure S3).[42] Theoretical modeling software was also used to simulate each *m/z* peak in Figure 2a, and the experimental data match favorably with simulated data (summarized in Table S1). For *C-2* (Figure 2b), *m/z* peaks are assigned to $Ag_xS_yNa_z$ (x = 5, 6, 7; y = 3–6; z = 0–6). This result may help us to understand the emission spectra of *C-2*. Previous studies reported the emission of Ag_5 and Ag_7 at 480 and 440 nm, respectively.[43,44] We deduced that the emission peak at 432 nm is attributed to the coupled effect of Ag_5 and Ag_7 and combine to create the blue broadened fluorescence spectrum of sample *C-2* in Figure 1b. MALDI-TOF mass spectra showed that the *CCYTAT* moiety could form different Ag clusters in strong and weak alkaline solutions. The mass spectra implied *C-1* is predominantly monodisperse Ag_{28}, while *C-2* includes Ag_5, Ag_6, and Ag_7 clusters.

Tyrosine is speculated to play an important role in reducing Ag^+ to Ag clusters. To verify this, the absorption of tyrosine and *CCYTAT* was studied. Absorption spectra of *C-1* and *C-2* are shown in Figure 3, in which the peptide transition is dominant in the 200–300 nm region. Figure 3a shows that absorption peaks of *CCYTAT* (black, pH ~7) occur at 223 and 275 nm. *C-1* (red, pH ~12) has a strong absorption peak at 242 nm and a weaker one at 290 nm, and *CCYTAT* (cyan, pH ~12) exhibits similar peaks to *C-1*. In Figure 3b, ***C-2*** (blue, pH ~9) and *CCYTAT* (green, pH ~9) have similar absorptions located at 223 and 242 nm and 275 and 298 nm, respectively. Upon comparing the absorption of tyrosine solutions (Figure S4) at 223 and 274 nm

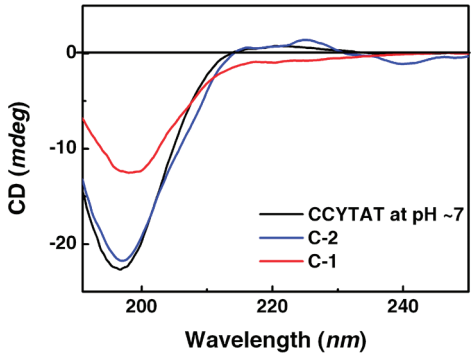

Figure 4. CD spectra of *C-1*, *C-2*, and pure *CCYTAT* at pH ~7. *CCYTAT* (black) has a strong negative peak at 197 nm and a weak positive peak at 220 nm, which are characteristic of a 3_1-helix. *C-2* (blue) has features similar to those for *CCYTAT*. *C-1* (red) shows a negative peak at 197 nm and a weak negative band at 220 nm.

(black, pH ~7) and at 240 and 294 nm (cyan, pH ~12), the absorption of *C-1* closely resembles that of oxidized tyrosine at pH ~12 (Figure S4, cyan). This indicates that phenolic peptide moieties are completely converted to phenoxide.[45] Only a fraction of the *C-2* peptide phenolic group is converted to phenoxide at pH ~9. A previous report disclosed that tyrosine played an important role in reducing $AgNO_3$, and tyrosine has different reductive ability when it is dissolved in aqueous solution at different pH values.[30,45] At pH ~12, tyrosine could strongly reduce Ag ions to Ag atoms, and more Ag atoms prefer to aggregate into a large Ag cluster, while at pH ~9, the reductive ability of tyrosine was weaker and small Ag clusters are preferred as reduced Ag atoms are in lower quantity.

In addition to the tyrosine reduction potential, the peptide structure may also have a role in forming different species. Circular dichroism (CD) spectra of *C-1*, *C-2*, and the free peptide are shown in Figure 4, with experimental details available in Supporting Information section S4. The spectrum of the *CCYTAT* solution (black, pH ~7) has a strong negative band at 197 nm and a weak positive band at 220 nm, which are characteristic of peptides with a 3_1-helical structure.[36] The CD

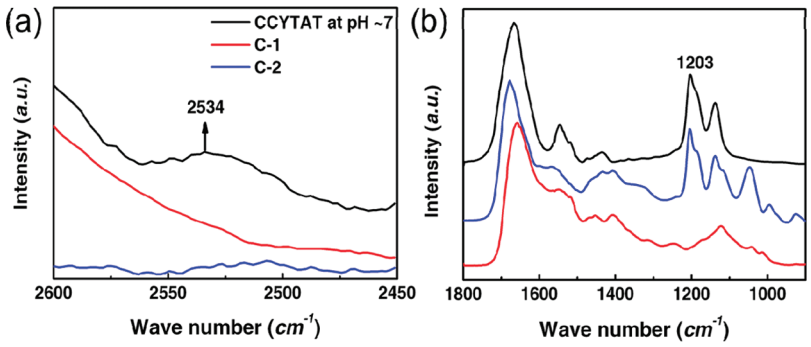

Figure 5. (a) IR spectra of the thiol group region for *CCYTAT*, *C-1*, and *C-2* at pH ~7. (b) IR spectra of *C-1* (red), *C-2* (blue), and *CCYTAT* (black, pH ~7) at 2000−1000 cm^{-1}. The 1203 cm^{-1} peak corresponds to vibration of the C−OH phenol group in *CCYTAT* (black), which is absent for *C-1* and weakened for *C-2*.

spectrum of *C-1* (red) shows a negative band at 219 nm accompanied by a stronger negative band at 200 nm; these are characteristic of an unordered peptide.[36] No obvious change is observed for *C-2* (blue), which suggests the *CCYTAT* peptide sequence retains a 3_1-helical structure. Thus, the CD results suggest that a strongly alkaline solution (pH ~12) converts the helical *CCYTAT* sequence of *C-1* into an unordered peptide.

The *CCYTAT* side chain has abundant lysine residues, and the change in pH may influence the peptides' secondary structure. The solution pH of ~12 is higher than the pK_a of the lysine side chain (~10.5), which induces lysine deprotonation and neutralizes the side chains. Electrostatic repulsion between peptide side chains decreases, which may cause the helical structure to become unordered. At pH ~9, the *C-2* peptide retains its helical structure.

The infrared (IR) spectra of the peptide may give information for understanding how the peptide anchors to the Ag cluster *via* the thiol group (Supporting Information section S5). Figure 5a shows the spectrum of *CCYTAT* (black, pH ~7), and the band at 2530 cm^{-1} is characteristic of the thiol stretching vibration. For *C-1* and *C-2* (red and blue, respectively), the thiol stretching vibration intensity weakens, which indicates that the thiol groups of *CCYTAT* interact with Ag clusters.[41,43]

In Figure 5b, the peak at 1203 cm^{-1} corresponds to the characteristic vibration of the C−OH phenol group of Tyr (black). This peak is absent in the spectrum of *C-1* (red), which indicates that phenol is converted to phenoxide. For *C-2* (blue), the peak at 1203 cm^{-1} weakens, indicating partial phenol conversion to phenoxide after alkaline treatment. The formation of phenoxide reflects the depletion of phenolic residues.[45] IR results are in agreement with the UV−visible absorption results in Figure 3, where the phenol and phenoxide groups of Tyr show different transitions when the peptide is in alkaline conditions.

CONCLUSIONS

Serial Ag clusters were synthesized using a single peptide sequence from different alkaline solutions. The peptide reduces Ag^+ to Ag clusters and anchor clusters *via* thiol groups. Serial Ag cluster formation is controlled by the pH-dependent reduction potential of Tyr and the pH-dependent peptide secondary structure. The peptide contains the cell nucleus targeting sequence *CCYTAT*; thus the as-synthesized Ag clusters have potential in cell imaging. The tunable emission of the peptide−cluster can aid the simultaneous multicolor staining of cells.

METHODS

Chemicals and Materials. Chemicals were obtained from Sigma-Aldrich unless otherwise mentioned. Ultrapure Millipore water (Milli-Q, 18.2 MΩ) was used in all experiments. The *CCYTAT* peptide was synthesized using a solid-phase method (China Peptides Co. Ltd., purity 95%). All glassware was washed with aqua regia (3:1 conc HCl/conc HNO_3) and then rinsed with ultrapure water and ethanol.

Peptide Biomineralized Ag Clusters. In a typical experiment, aqueous $AgNO_3$ (25 mM, 16 μL) was slowly introduced into a solution of *CCYTAT* (1.06 mM, 376 μL) in a 5 mL vial under vigorous stirring. NaOH (0.5 M, 8 μL) was added within 30 s to adjust the final pH to ~12. The sample was sealed and stored at 37 °C in the dark for 8 h without disturbance. The as-synthesized mixture was dialyzed for 12 h (dialysis tube MWCO 500) and then concentrated using a dialysis tube (Merck, Midi D-tube, MWCO 3000, 50−800 μL) to remove any reagents and free *CCYTAT*. Red-emitting Ag clusters were obtained.

To prepare blue-emitting Ag clusters, an analogous procedure was used except NaOH (0.5 M, 1.6 μL) was added to give a final pH of ~9, and the solution was stored at 37 °C for three days. The sample was filtered (13 mm, 0.22 μm/W) and then dialyzed as above.

Acknowledgment. This work was supported by the 973 Program (2007CB935604, 2009CB930204, 2011CB933400), NSFC (30870677, 31070891), and CAS Knowledge Innovation Program.

Supporting Information Available: Experimental details regarding collection of photoluminescence spectra, quantum yield, MALDI-TOF mass spectra, UV−visible absorption spectra, CD spectra, and IR spectra. This material is available free of charge *via* the Internet at http://pubs.acs.org.

REFERENCES AND NOTES

1. Zheng, J.; Nicovich, P. R.; Dickson, R. M. Highly Fluorescent Noble-Metal Quantum Dots. *Annu. Rev. Phys. Chem.* **2007**, *58*, 409–431.
2. Zheng, J.; Dickson, R. M. Individual Water-Soluble Dendrimer-Encapsulated Silver Nanodot Fluorescence. *J. Am. Chem. Soc.* **2002**, *124*, 13982–13983.
3. Guo, W.; Yuan, J.; Wang, E. Oligonucleotide-Stabilized Ag Nanoclusters as Novel Fluorescence Probes for the Highly Selective and Sensitive Detection of the Hg^{2+} Ion. *Chem. Commun.* **2009**, *2009*, 3395–3397.
4. Lee, T. H.; Gonzalez, J. I.; Zheng, J.; Dickson, R. M. Single-Molecule Optoelectronics. *Acc. Chem. Res.* **2004**, *38*, 534–541.
5. Vosch, T.; Antoku, Y.; Hsiang, J. C.; Richards, C. I.; Gonzalez, J. I.; Dickson, R. M. Strongly Emissive Individual DNA-Encapsulated Ag Nanoclusters as Single-Molecule Fluorophores. *Proc. Natl. Acad. Sci. U. S. A.* **2007**, *104*, 12616.
6. Yu, J.; Choi, S.; Richards, C. I.; Antoku, Y.; Dickson, R. M. Live Cell Surface Labeling with Fluorescent Ag Nanocluster Conjugates. *Photochem. Photobiol.* **2008**, *84*, 1435–1439.
7. Shang, L.; Dong, S. Sensitive Detection of Cysteine Based on Fluorescent Silver Clusters. *Biosens. Bioelectron.* **2009**, *24*, 1569–1573.
8. Richards, C. I.; Choi, S.; Hsiang, J. C.; Antoku, Y.; Vosch, T.; Bongiorno, A.; Tzeng, Y. L.; Dickson, R. M. Oligonucleotide-Stabilized Ag Nanocluster Fluorophores. *J. Am. Chem. Soc.* **2008**, *130*, 5038–5039.
9. Makarava, N.; Parfenov, A.; Baskakov, I. V. Water-Soluble Hybrid Nanoclusters with Extra Bright and Photostable Emissions: A New Tool for Biological Imaging. *Biophys. J.* **2005**, *89*, 572–580.
10. Yu, J.; Choi, S.; Dickson, R. M. Shuttle-Based Fluorogenic Silver-Cluster Biolabels. *Angew. Chem., Int. Ed.* **2009**, *48*, 318–320.
11. Xu, H.; Suslick, K. S. Sonochemical Synthesis of Highly Fluorescent Ag Nanoclusters. *ACS Nano* **2010**, *4*, 3209–3214.
12. Zheng, J.; Petty, J. T.; Dickson, R. M. High Quantum Yield Blue Emission from Water-Soluble Au_8 Nanodots. *J. Am. Chem. Soc.* **2003**, *125*, 7780–7781.
13. Shichibu, Y.; Konishi, K. HCl-Induced Nuclearity Convergence in Diphosphine-Protected Ultrasmall Gold Clusters: A Novel Synthetic Route to "Magic-Number" Au_{13} Clusters. *Small* **2010**, *6*, 1216–1220.
14. Zhu, M.; Lanni, E.; Garg, N.; Bier, M. E.; Jin, R. Kinetically Controlled, High-Yield Synthesis of Au_{25} Clusters. *J. Am. Chem. Soc.* **2008**, *130*, 1138–1139.
15. Wu, Z.; Suhan, J.; Jin, R. One-Pot Synthesis of Atomically Monodisperse, Thiol-Functionalized Au_{25} Nanoclusters. *J. Mater. Chem.* **2008**, *19*, 622–626.
16. Lee, D.; Donkers, R. L.; Wang, G.; Harper, A. S.; Murray, R. W. Electrochemistry and Optical Absorbance and Luminescence of Molecule-Like Au_{38} Nanoparticles. *J. Am. Chem. Soc.* **2004**, *126*, 6193–6199.
17. Fedrigo, S.; Harbich, W.; Buttet, J. Optical Response of Ag_2, Ag_3, Au_2, and Au_3 in Argon Matrices. *J. Chem. Phys.* **1993**, *99*, 5712–5717.
18. Peyser, L. A.; Vinson, A. E.; Bartko, A. P.; Dickson, R. M. Photoactivated Fluorescence from Individual Silver Nanoclusters. *Science* **2001**, *291*, 103.
19. Branham, M. R.; Douglas, A. D.; Allan, J.; Tracy, J. B.; White, P. S.; Murray, R. W. Arylthiolate-Protected Silver Quantum Dots. *Langmuir* **2006**, *22*, 11376–11383.
20. Ritchie, C. M.; Johnsen, K. R.; Kiser, J. R.; Antoku, Y.; Dickson, R. M.; Petty, J. T. Ag Nanocluster Formation Using a Cytosine Oligonucleotide Template. *J. Phys. Chem. C* **2006**, *111*, 175–181.
21. Petty, J. T.; Fan, C.; Story, S. P.; Sengupta, B.; St. John Iyer, A.; Prudowsky, Z.; Dickson, R. M. DNA Encapsulation of 10 Silver Atoms Producing a Bright, Modulatable, Near-Infrared-Emitting Cluster. *J. Phys. Chem. Lett.* **2010**, *1*, 2524–2529.
22. Petty, J. T.; Zheng, J.; Nicholas, V.; Dickson, R. M. DNA-Templated Ag Nanocluster Formation. *J. Am. Chem. Soc.* **2004**, *126*, 5207–5212.
23. Sengupta, B.; Ritchie, C. M.; Buckman, J. G.; Johnsen, K. R.; Goodwin, P. M.; Petty, J. T. Base-Directed Formation of Fluorescent Silver Clusters. *J. Phys. Chem. C* **2008**, *112*, 18776–18782.
24. Koszinowski, K.; Ballweg, K. A Highly Charged Ag_6^{4+} Core in a DNA-Encapsulated Silver Nanocluster. *Chem.—Eur. J.* **2010**, *16*, 3285–3290.
25. Grohn, F.; Bauer, B. J.; Akpalu, Y. A.; Jackson, C. L.; Amis, E. J. Dendrimer Templates for the Formation of Gold Nanoclusters. *Macromolecules* **2000**, *33*, 6042–6050.
26. Sun, X.; Dong, S.; Wang, E. One-Step Preparation and Characterization of Poly(propyleneimine) Dendrimer-Protected Silver Nanoclusters. *Macromolecules* **2004**, *37*, 7105–7108.
27. Yu, J.; Patel, S. A.; Dickson, R. M. In Vitro and Intracellular Production of Peptide-Encapsulated Fluorescent Silver Nanoclusters. *Angew. Chem., Ger. Ed.* **2007**, *119*, 2074–2076.
28. Mitric, R.; Petersen, J.; Kulesza, A.; Bonacic-Kouteck, V.; Tabarin, T.; Compagnon, I.; Antoine, R.; Broyer, M.; Dugourd, P. Absorption Properties of Cationic Silver Cluster-Tryptophan Complexes: A Model for Photoabsorption and Photoemission Enhancement in Nanoparticle-Biomolecule Systems. *Chem. Phys.* **2008**, *343*, 372–380.
29. Díez, I.; Ras, R. H. A. Few-Atom Silver Clusters as Fluorescent Reporters. In *Advanced Fluorescence Reporters in Chemistry and Biology II*; Demchenko, A. P., Ed.; Springer: Berlin, 2010; pp 307—332.
30. Xie, J.; Zheng, Y.; Ying, J. Y. Protein-Directed Synthesis of Highly Fluorescent Gold Nanoclusters. *J. Am. Chem. Soc.* **2009**, *131*, 888–889.
31. Dickerson, M. B.; Sandhage, K. H.; Naik, R. R. Protein-and Peptide-Directed Syntheses of Inorganic Materials. *Chem. Rev.* **2008**, *108*, 4935–4978.
32. Naik, R. R.; Stringer, S. J.; Agarwal, G.; Jones, S. E.; Stone, M. O. Biomimetic Synthesis and Patterning of Silver Nanoparticles. *Nat. Mater.* **2002**, *1*, 169–172.
33. Cui, R.; Liu, H. H.; Xie, H. Y.; Zhang, Z. L.; Yang, Y. R.; Pang, D. W.; Xie, Z. X.; Chen, B. B.; Hu, B.; Shen, P. Living Yeast Cells as a Controllable Biosynthesizer for Fluorescent Quantum Dots. *Adv. Funct. Mater.* **2009**, *19*, 2359–2364.
34. Raveendran, P.; Fu, J.; Wallen, S. L. Completely "Green" Synthesis and Stabilization of Metal Nanoparticles. *J. Am. Chem. Soc.* **2003**, *125*, 13940–13941.
35. Vivès, E.; Brodin, P.; Lebleu, B. A Truncated HIV-1 Tat Protein Basic Domain Rapidly Translocates through the Plasma Membrane and Accumulates in the Cell Nucleus. *J. Biol. Chem.* **1997**, *272*, 16010–16017.
36. Ruzza, P.; Calderan, A.; Guiotto, A.; Osler, A.; Borin, G. Tat Cell-Penetrating Peptide Has the Characteristics of a Poly (proline) II Helix in Aqueous Solution and in SDS Micelles. *J. Pept. Sci.* **2004**, *10*, 423–426.
37. Efthymiadis, A.; Briggs, L. J.; Jans, D. A. The HIV-1 Tat Nuclear Localization Sequence Confers Novel Nuclear Import Properties. *J. Biol. Chem.* **1998**, *273*, 1623–1628.
38. Nori, A.; Jensen, K. D.; Tijerina, M.; Kopeckova, P.; Kopecek, J. Tat-Conjugated Synthetic Macromolecules Facilitate Cytoplasmic Drug Delivery to Human Ovarian Carcinoma Cells. *Bioconjugate Chem.* **2003**, *14*, 44–50.
39. Cathcart, N.; Mistry, P.; Makra, C.; Pietrobon, B.; Coombs, N.; Jelokhani-Niaraki, M.; Kitaev, V. Chiral Thiol-Stabilized Silver Nanoclusters with Well-Resolved Optical Transitions Synthesized by a Facile Etching Procedure in Aqueous Solutions. *Langmuir* **2009**, *25*, 5840–5846.
40. Wu, Z.; Lanni, E.; Chen, W.; Bier, M. E.; Ly, D.; Jin, R. High Yield, Large Scale Synthesis of Thiolate-Protected Ag_7 Clusters. *J. Am. Chem. Soc.* **2009**, *131*, 16672–16674.
41. Adhikari, B.; Banerjee, A. Facile Synthesis of Water-Soluble Fluorescent Silver Nanoclusters and HgII Sensing. *Chem. Mater.* **2010**, *22*, 4364–4371.
42. Arnold, R. J.; Reilly, J. P. High-Resolution Time-of-Flight Mass Spectra of Alkanethiolate-Coated Gold Nanocrystals. *J. Am. Chem. Soc.* **1998**, *120*, 1528–1532.
43. Rao, T. U. B.; Pradeep, T. Luminescent Ag_7 and Ag_8 Clusters by Interfacial Synthesis. *Angew. Chem., Int. Ed.* **2010**, *49*, 3925.

44. Antoku, Y. Fluorescent Polycytosine-Encapsulated Silver Nanoclusters. Ph.D. thesis, Georgia Institute of Technology, Atlanta, May 2007.
45. Xie, J.; Lee, J. Y.; Wang, D. I. C.; Ting, Y. P. Silver Nanoplates: From Biological to Biomimetic Synthesis. *ACS Nano* **2007**, *1*, 429–439.